Received: 14 July 2016 | Revised: 3 August 2016 | Accepted: 19 August 2016

DOI 10.1002/aoc.3624

WILEY Applied Organometallic Chemistry

FULL PAPER

Au- and Ag-loaded MnO_2 nanostructures supported on nitrogen- and nitrogen–sulfur-doped pyroproteins: Synthesis and catalytic activity in organic transformations

Zeinab Hezarkhani | Ahmad Shaabani*

Faculty of Chemistry, Shahid Beheshti University, GC, PO Box 19396-4716 Tehran, Iran

Correspondence
Ahmad Shaabani, Faculty of Chemistry, Shahid Beheshti University, GC, PO Box 19396-4716, Tehran, Iran.
Email: a-shaabani@sbu.ac.ir

Four novel Au- and Ag-loaded MnO_2 nanostructures supported on nitrogen-doped pyroprotein of natural silk (Au–MnO_2@PPNS and Ag–MnO_2@PPNS) and nitrogen–sulfur-doped pyroprotein of natural wool (Au–MnO_2@PPNW and Ag–MnO_2@PPNW) have been synthesized. Nitrogen- and nitrogen–sulfur-doped pyroproteins were prepared by carbonization of natural silk and wool proteins, respectively. The catalysts were investigated for the aerobic oxidation of aromatic hydrocarbons of petroleum naphtha and the aerobic oxidative synthesis of 2-phenylbenzo[*d*]thiazoles, 2-phenyl-1*H*-benzo[*d*]imidazoles and 2-phenyl-4-quinazolinones in the absence of any co-promoter and additional oxidizing reagent. The prepared catalytic systems showed higher catalytic activity in comparison to aggregated catalysts.

KEYWORDS

MnO_2 nanostructures, natural silk, natural wool, nitrogen- and nitrogen–sulfur-doped carbon, pyroprotein

1 | INTRODUCTION

Manganese dioxide (MnO_2) as an abundant, low-toxicity and environmentally friendly reagent has attracted much attention because of its physical and chemical properties and wide range of applications in oxidation catalysis.[1–5] Impurity doping as an effective method for manipulating the physical and chemical properties of catalysts could be done by non-equilibrium doping with an appropriate metal.[6,7] Recently, gold-doped and silver-doped MnO_2 were shown to have a significantly improved performance compared with undoped MnO_2.[8–10] The specific surface area of catalytic materials has an obvious influence on the performance of catalysts.[11,12] Consequently, doped MnO_2 nanostructures not only have distinctive physicochemical properties, associated with a large specific surface area of dimensions on the nanometre scale, but also appropriate metal doping.[13]

Various amino acids link via peptide bonds with each other to create proteins. Each peptide has specific characteristics and the linking of specific sequences of amino acids via the peptide bonds leads to individual secondary structures. The β-sheets are the most stable secondary structures. The interchain hydrogen bonding between adjacent amino acids in the peptide blocks causes the formation of the β-sheet structures. This property is obviously observable in natural protein fibres such as silk (Scheme 1).[14] The α-helices are the usual secondary structure of proteins. In this conformation the N─H group in the backbone hydrogen bonds to the C═O group of the backbone, four residues earlier. Such a structure is observable in the polypeptide chain of wool (Scheme 1).[14] Due to the secondary structures of various natural protein-rich materials, the behaviours of them are different in the process of pyrolysis.

The nitrogen atoms included in nitrogen-containing carbon compounds improve the properties of the bulk carbons which increases the applications suggested for these carbon-containing materials. Varying the amounts of nitrogen can be used to alter the properties of the materials, and most of the time a higher amount of nitrogen improves the specific properties.[15] The pyrolysis of nitrogen-rich biopolymers is one of the most appropriate processes for the synthesis of the mentioned materials.[16–18]

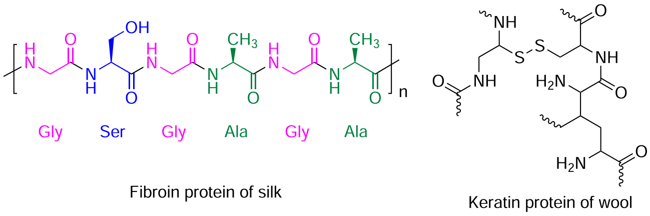

Fibroin protein of silk

Keratin protein of wool

SCHEME 1 Structure of proteins of silk and wool.

Silk and wool proteins have unique biological functionality and they are of great interest to the scientific community. Therefore in the study presented here the pyrolysis of silk and wool proteins was used to obtain nitrogen-doped pyroproteins and their usability as catalyst supports for organic transformations was investigated. Because of our ongoing interest in developing new MnO_2-containing catalytic systems for organic reactions,[19–23] herein we report the synthesis of Au–MnO_2 and Ag–MnO_2 nanostructures supported on nitrogen- and nitrogen–sulfur-doped pyroproteins prepared by pyrolysis of natural silk and wool proteins, respectively. We investigated their catalytic activity in the one-pot tandem aerobic oxidative two-component synthesis of organic compounds.

2 | EXPERIMENTAL

2.1 | Synthesis of N-doped pyroprotein of natural silk (PPNS) and N,S-doped pyroprotein of natural wool (PPNW)

Regenerated silk fibroin (RSF) was prepared as described elsewhere.[16,24] Briefly, to extract the silk sericin, wax and impurities, natural silkworm cocoons were boiled for 30 min in an aqueous solution of 5% (*w*/*v*) Na_2CO_3. The extracted silk fibroin was washed with deionized water several times and dried at room temperature for two days. The prepared silk fibroin fibres were dissolved into a 9.3 M LiBr solution at 60°C for 6 h. The obtained silk fibroin solution was dialyzed in deionized water for three days and centrifuged at 7000 rpm for about 10 min to remove insoluble impurities. Finally, the solvent was evaporated to afford RSF.

To prepare regenerated wool keratin (RWK), a method similar to that of a previous report was used.[25] Briefly, to 3.0 g of 1-butyl-3-methylimidazolium chloride ([BMIM]Cl) was added 75 mg of natural wool fibres. The reaction mixture was heated at 130°C under a nitrogen atmosphere. The reaction mixture was stirred magnetically until the natural wool fibres were completely dissolved. Addition of water (50 ml) to the [BMIM]Cl solution was done for precipitation and regeneration of the dissolved wool keratin. The wool keratin precipitate was separated via centrifugation (8000 rpm for 20 min). RWK was washed with water (using a centrifuge) to remove any ionic liquid that may be retained in the RWK. The obtained RWK was dried under vacuum at 45°C during three days.

The prepared RSF and RWK were heated to 500°C with a controlled heating programme in a tubular furnace under a nitrogen atmosphere. The carbonization process was done in three steps. The silk fibroin proteins and wool keratin proteins were rapidly heated to 100°C and maintained at this temperature for 1 h to remove the absorbed water. The temperature of the samples was increased from 100 to 500°C at 5°C min^{-1}). The samples were maintained at 500°C for 5 h to induce the formation of the corresponding PPNS and PPNW. The prepared PPNS and PPNW were thoroughly ground at room temperature using a pestle.

2.2 | Synthesis of Au–MnO_2 and Ag–MnO_2 nanostructures supported on PPNS (Au–MnO_2@PPNS and Ag–MnO_2@PPNS) and PPNW (Au–MnO_2@PPNW and Ag-MnO_2@PPNW)

A mixture of pyroprotein powder (0.5 g) in 50 ml of water was prepared and sonicated for 30 min. The temperature of the mixture was raised to 60°C. A solution of $MnCl_2$ (0.02 M, 30 ml) at 70°C and a solution of $KMnO_4$ (0.01 M, 40 ml) at 60°C were prepared, separately. The as-prepared solutions of $KMnO_4$ and $MnCl_2$ were added dropwise to the mixture of pyroprotein powder with sonication during

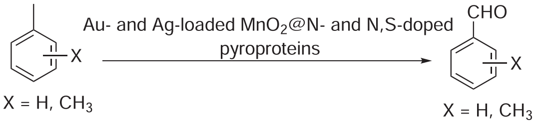

SCHEME 2 Aerobic oxidation of aromatic hydrocarbons of petroleum naphtha (toluene and three isomers of xylene) catalysed by Au–MnO_2@PPNS, Ag–MnO_2@PPNS, Au–MnO_2@PPNW and Ag–MnO_2@PPNW.

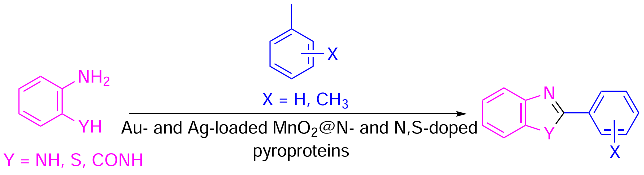

SCHEME 3 Oxidative synthesis of 2-arylbenzo[*d*]thiazole, 2-aryl-1*H*-benzo[*d*]imidazole and 2-aryl-4-quinazolinone derivatives catalysed by Au–MnO_2@PPNS, Ag–MnO_2@PPNS, Au–MnO_2@PPNW and Ag–MnO_2@PPNW.

TABLE 1 Amounts of carbon, nitrogen and sulfur in prepared PPNS and PPNW

	N-doped pyroprotein of natural silk	N,S-doped pyroprotein of natural wool
Carbon (%)	80.2	82.1
Nitrogen (%)	7.7	8.3
Sulfur (%)	—	0.9

3 h at 60°C. Finally, the mixture was filtered and the residue was washed successively with water (3 × 10 ml) and EtOH (3 × 10 ml) and dried under vacuum at 60°C to afford MnO_2@PPNS and MnO_2@PPNW.

For the synthesis of Au–MnO_2 and Ag–MnO_2 nanostructures supported on N- and N,S-doped pyroproteins, the modified method similar to that of previous reports[9,10] was used. A mixture of MnO_2@PPNS or MnO_2@PPNW (0.3 g) in

TABLE 2 Amounts of Au, Ag and MnO_2 in prepared catalysts

	MnO_2@PPNS	Au–MnO_2@PPNS	Ag–MnO_2@PPNS	MnO_2@PPNW	Au–MnO_2@PPNW	Ag–MnO_2@PPNW
Au (%)	—	0.11	—	—	0.20	—
MnO_2 (%)	7.68	7.66	7.63	8.07	8.04	8.03
Ag (%)	—	—	0.34	—	—	0.41

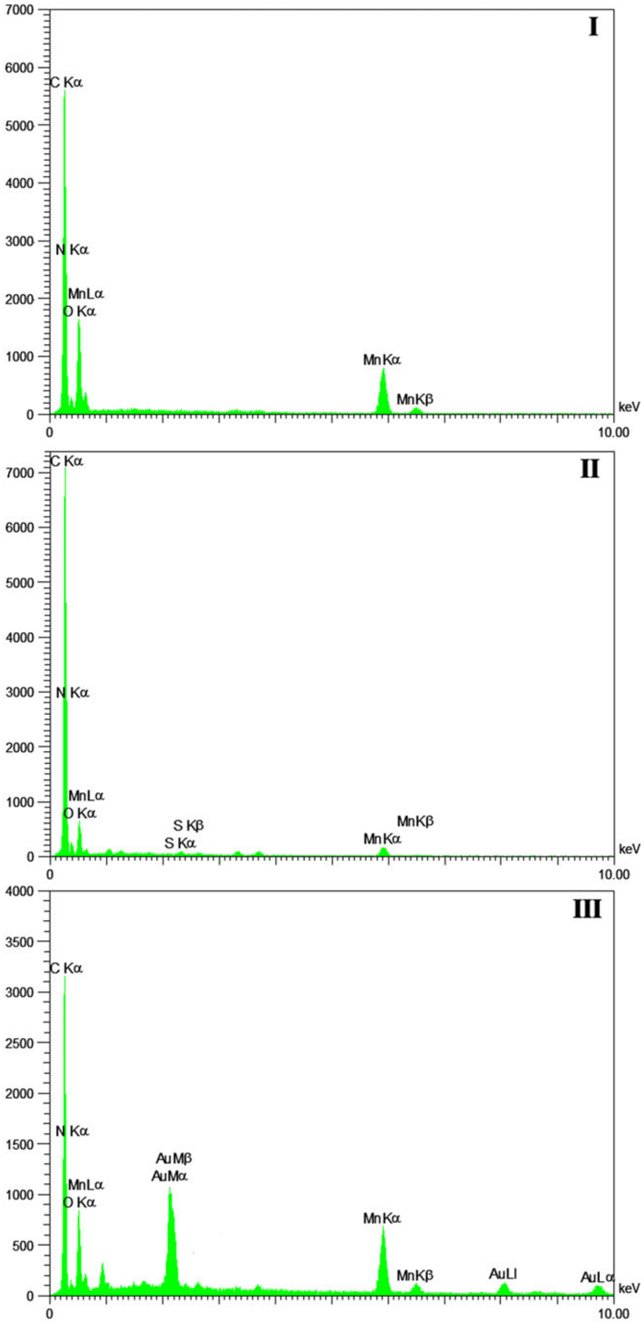

FIGURE 1 SEM–EDS results for MnO_2@PPNS (I), MnO_2@PPNW (II), Au–MnO_2@PPNS (III), Au–MnO_2@PPNW (IV), Ag–MnO_2@PPNS (V) and Ag–MnO_2@PPNW (VI).

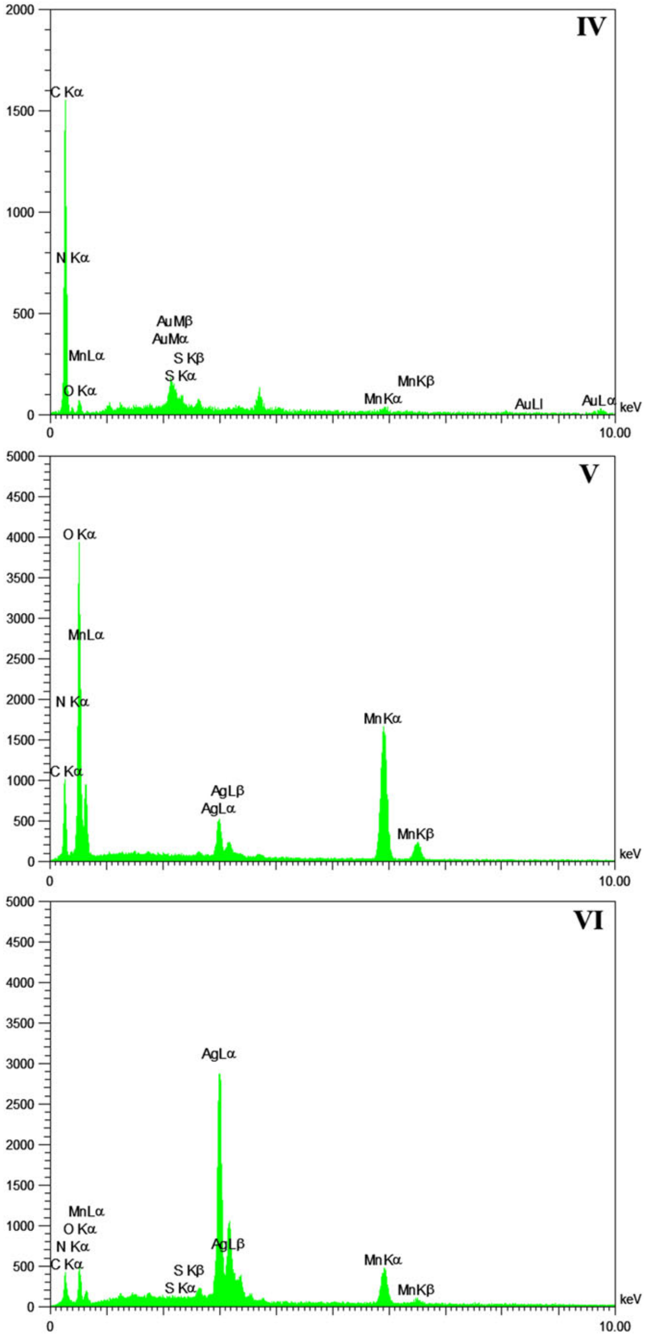

FIGURE 1 (Continued)

20 ml of water was sonicated for 30 min. An aqueous solution of $HAuCl_4$ (1.6 ml, 10 mM) was added to the prepared mixture and the mixture was stirred magnetically for 48 h. Then, the reaction mixture was centrifuged and the residue was collected. The prepared solid was redispersed in distilled water (10 ml). An aqueous solution of $NaBH_4$ (0.8 ml, 0.1 mM) was added to the mixture and the reaction medium was stirred magnetically for 4 h. The mixture was centrifuged to obtain the Au–MnO_2@PPNS and Au–MnO_2@PPNW catalysts.

To prepare the Ag–MnO_2@PPNS and Ag–MnO_2@PPNW catalysts, a similar method was used but with $AgNO_3$ (1.6 ml, 20 mM) instead of $HAuCl_4$.

2.3 | Oxidation of toluene or xylene: general procedure

To obtain the desired product (Scheme 2), toluene or xylene (8.0 ml) and the catalyst prepared as described in Section 2.2 were added to a two-necked flask. The reaction medium was stirred magnetically under reflux conditions for the required times. Air was bubbled into the reaction mixture at a rate of 5 ml min^{-1}. The progress of the reaction was monitored using GC and TLC. After completion of the reaction, the catalyst was separated using filtration and washed with ethanol. The product was identified using NMR analysis and quantified using GC with 1-dodecane as internal standard.

2.4 | General procedure for preparation of products **3a–d**, **5a–d** and **7a–d**

To obtain the desired product (Scheme 3), in a two-necked flask containing toluene or xylene (10 ml), an amine source (1.0 mmol) and the catalyst were added. The reaction medium was stirred under reflux conditions for the required times. Air was bubbled into the reaction mixture at a rate of 5 ml min^{-1}. The progress of the reaction was monitored using TLC. After completion of the reaction, the catalyst was separated from the reaction medium via filtration and washed with ethanol. Then the product was isolated using

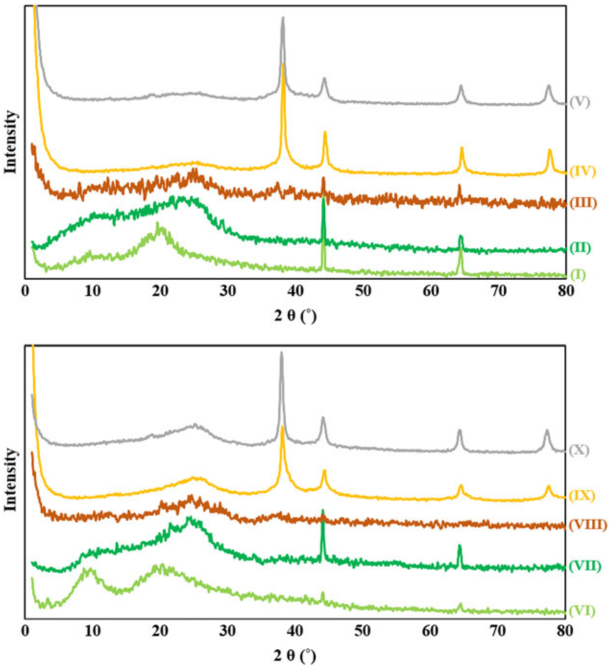

FIGURE 3 XRD patterns of natural silk (I), PPNS (II), MnO_2@PPNS (III), Au–MnO_2@PPNS (IV), Ag–MnO_2@PPNS (V), natural wool (VI), PPNW (VII), MnO_2@PPNW (VIII), Au–MnO_2@PPNW (IX) and Ag–MnO_2@PPNW (X).

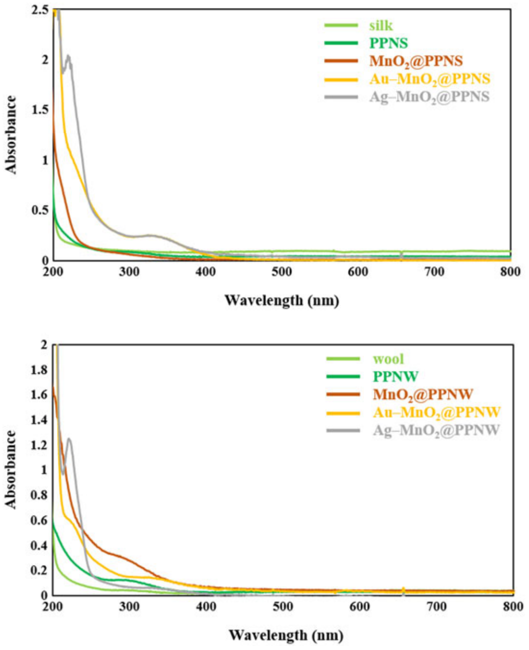

FIGURE 2 UV–visible spectra of natural silk, PPNS, MnO_2@PPNS, Au–MnO_2@PPNS, Ag–MnO_2@PPNS, natural wool, PPNW, MnO_2@PPNW, Au–MnO_2@PPNW and Ag–MnO_2@PPNW in water–aqua regia (10:1).

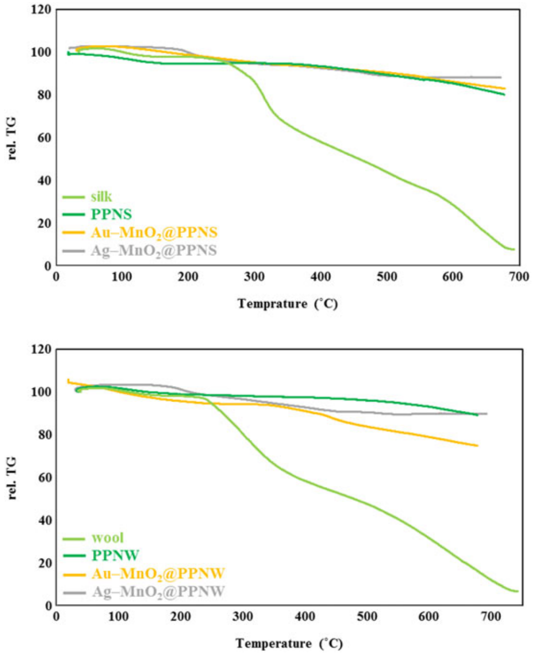

FIGURE 4 TGA curves of natural silk, PPNS, Au–MnO_2@PPNS, Ag–MnO_2@PPNS, natural wool, PPNW, Au–MnO_2@PPNW and Ag–MnO_2@PPNW in air.

column chromatography (ethyl acetate–*n*-hexane; 2:1). The product was identified using IR, ^{1}H NMR and ^{13}C NMR spectral analyses and quantified by isolated yield. The characterization data are provided in the supporting information.

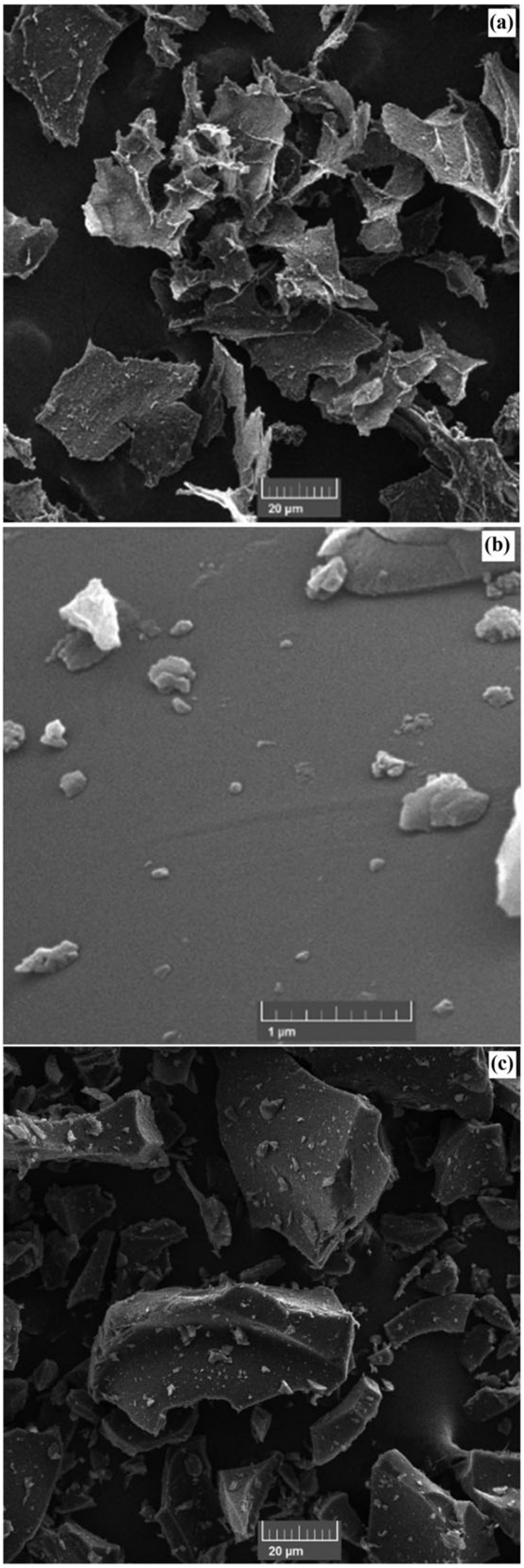

FIGURE 5 SEM images of PPNS (a, b), PPNW (c, d), Au–MnO_2@PPNS (e, f), Ag–MnO_2@PPNS (g, h), Au–MnO_2@PPNW (i, j) and Ag–MnO_2@PPNW (k, l).

3 | RESULTS AND DISCUSSION

The carbon, nitrogen, and sulfur contents of the silk protein- and wool protein-derived carbons were determined using elemental analysis (Table 1). The amounts of Au, Ag and Mn in the catalysts were determined using the flame atomic

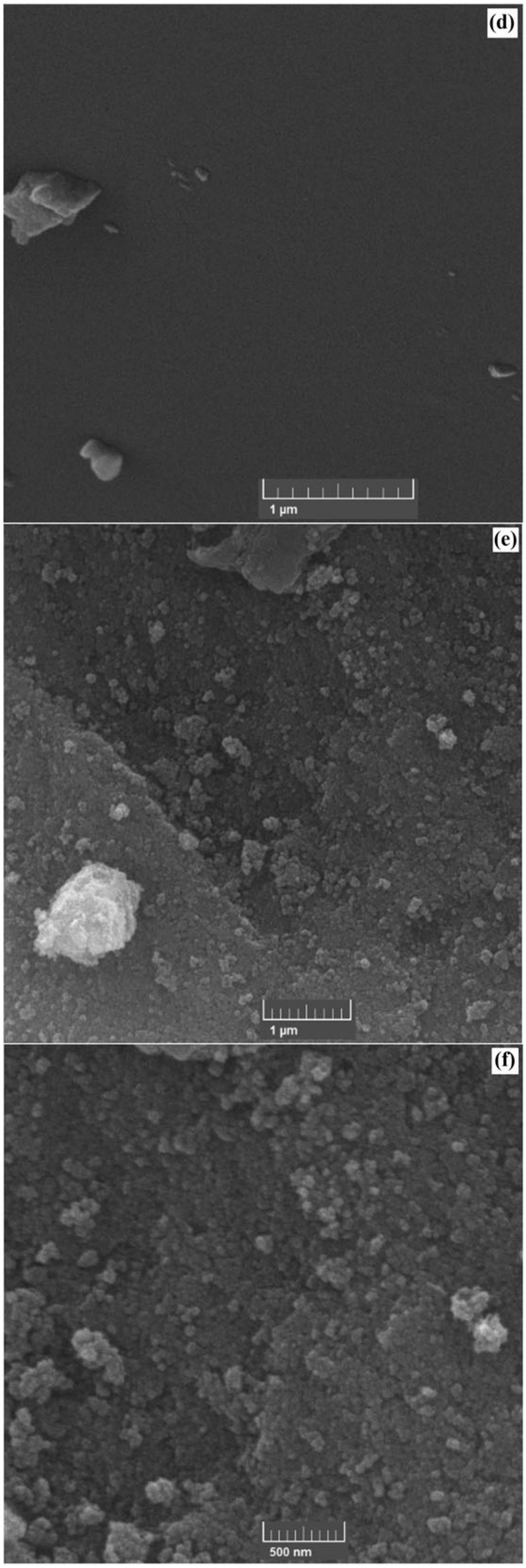

FIGURE 5 (Continued)

absorption spectroscopy and inductively coupled plasma optical emission spectrometry methods. The results of the analysis are presented in Table 2.

For the determination of the chemical composition of MnO_2@PPNS, MnO_2@PPNW, Au–MnO_2@PPNS, Ag–MnO_2@PPNS, Au–MnO_2@PPNW and Ag–MnO_2@PPNW, the energy dispersive spectroscopy (EDS) method was applied (Figure 1).

UV–visible spectral analysis of natural silk, PPNS, MnO_2@PPNS, Au–MnO_2@PPNS, Ag–MnO_2@PPNS, natural wool, PPNW, MnO_2@PPNW, Au–MnO_2@PPNW and Ag–MnO_2@PPNW was also conducted (Figure 2). For this

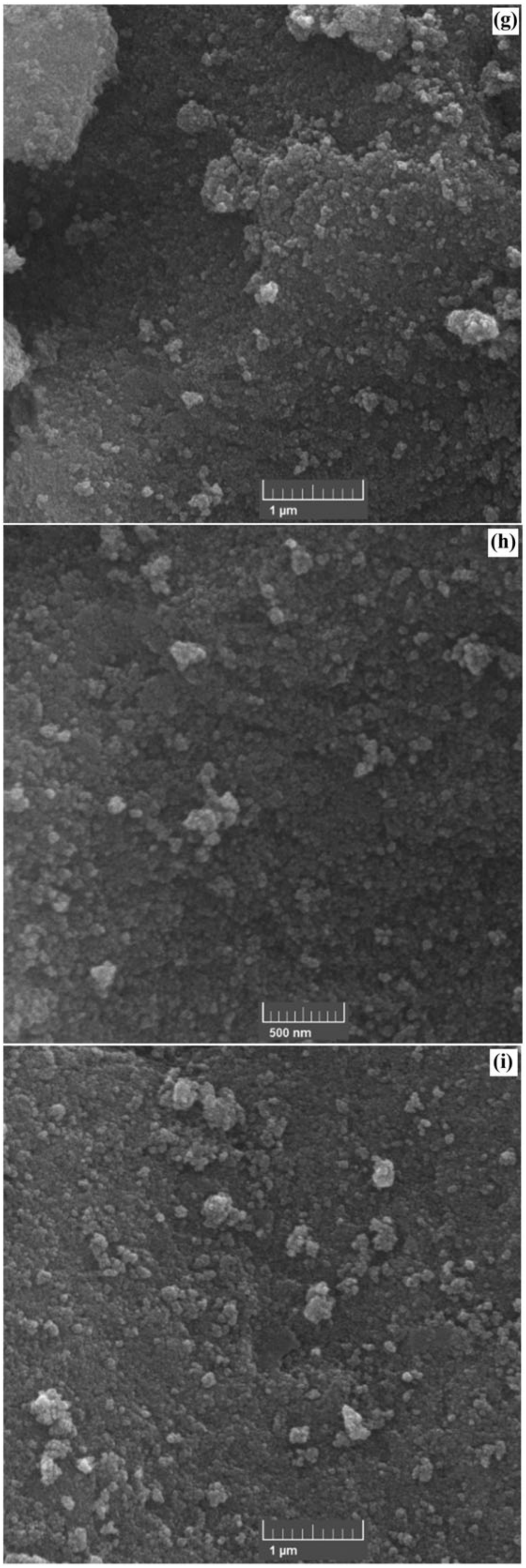

FIGURE 5 (Continued)

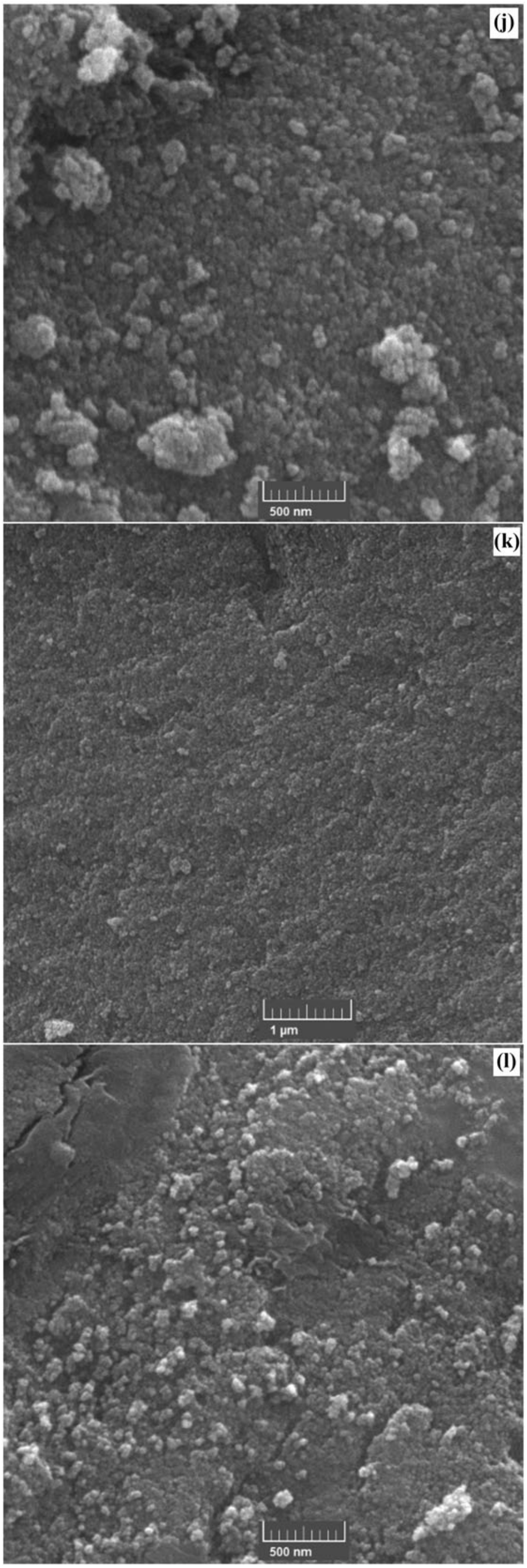

FIGURE 5 (Continued)

analysis the prepared catalysts were dissolved in aqua regia (concentrated HCl–concentrated HNO_3 at 3:1) and then diluted with deionized water.

The X-ray diffraction (XRD) patterns of the initial natural silk and wool, of PPNS and PPNW and of the prepared catalysts were employed to study the structure of the catalysts. The two broad peaks at 2θ of around 9.5° and 19.5° are related to the silk fibres (Figure 3-I). The pattern of wool has two characteristic broad peaks at 2θ of 9° and 21° (Figure 3-VI). PPNS and PPNW show specific peaks different from those of the original parent natural biopolymers (Figure 3-II and VII). For PPNS the characteristic broad peaks at 2θ of 10° and 21° and for PPNW at 2θ of 10.5° and 24° are observable. In the case of MnO_2@PPNS and MnO_2@PPNW, PPNS and PPNW show very strong peaks which means that the peaks related to MnO_2 cannot be observed because of very weak peaks of MnO_2 moieties. In addition, the observations imply that the nature of the PPNS and PPNW supports is not altered during the process of the preparation of the MnO_2@PPNS and MnO_2@PPNW catalytic systems (Figure 3-III and VIII).

The Au-loaded structure of MnO_2 nanostructures in Au–MnO_2@PPNS and Au–MnO_2@PPNW nanocatalysts was confirmed through powder XRD according to a previous report.[8] Also, the XRD patterns of Ag–MnO_2@PPNS and Ag–MnO_2@PPNW nanocatalysts show the characteristics of an Ag-loaded structure of MnO_2 nanostructures.[9,10]

The thermal behaviour of the prepared catalytic systems was studied using thermogravimetric analysis (TGA). From the TGA data (Figure 4) it is clear that both natural silk and wool show two decomposition stages. The results of TGA of PPNS and PPNW show that they have very high thermal stability in comparison with the parent materials. Also, the prepared Au–MnO_2@PPNS, Ag–MnO_2@PPNS, Au–MnO_2@PPNW and Ag–MnO_2@PPNW show high thermal stability as can be seen from Figure 4.

Scanning electron microscopy (SEM) and transmission electron microscopy (TEM) were used to study the morphology and the structure of the prepared catalytic systems (Figures 5 and 6). From the SEM and TEM results it is observed that the Au–MnO_2 and Ag–MnO_2 nanostructures are dispersed uniformly on the surface of the prepared PPNS and PPNW supports.

Since selective oxidation of primary C—H bonds with air is of fundamental importance for the sustainable exploitation of available feedstocks, the catalytic activity of the prepared catalysts was studied in the aerobic oxidation of aromatic hydrocarbons of petroleum naphtha (toluene and three isomers of xylene) (Scheme 2).

To achieve a suitable catalytic system for the mentioned reactions, we examined Au–MnO_2@PPNS, Ag–MnO_2@PPNS, Au–MnO_2@PPNW and Ag–MnO_2@PPNW catalysts in the reaction media. Aerobic oxidation of toluene was selected as a model reaction (Table 3). From the results presented in Table 3 (entries 1 and 11) it can be seen that

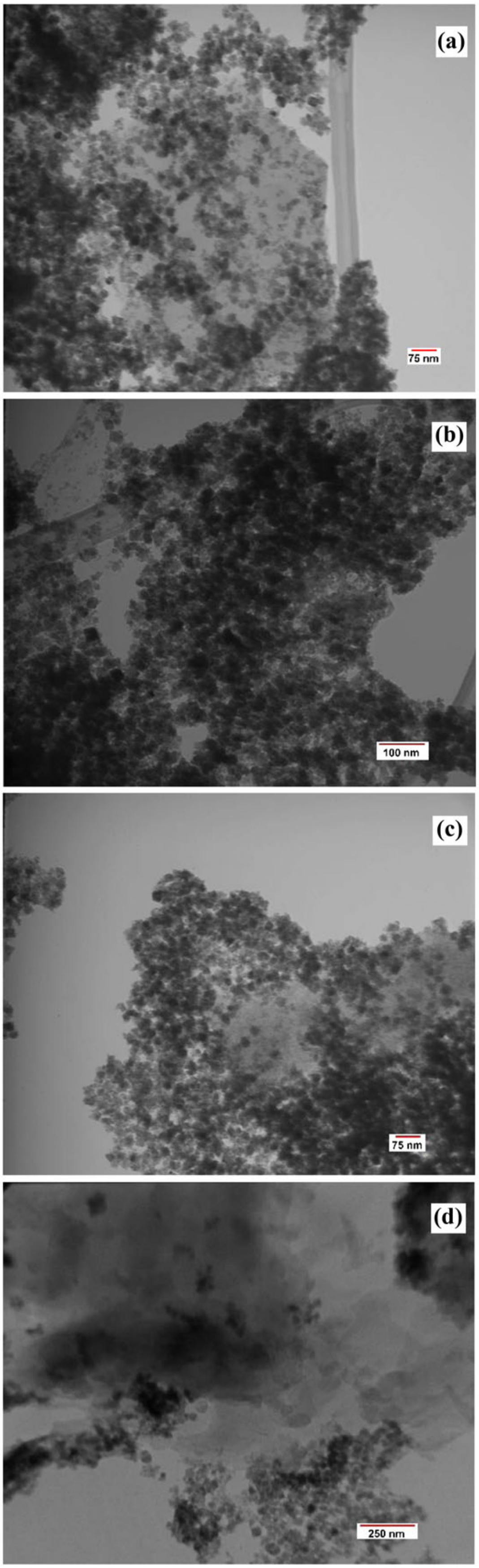

FIGURE 6 TEM images of Au–MnO_2@PPNS (a), Ag–MnO_2@PPNS (b), Au–MnO_2@PPNW (c) and Ag–MnO_2@PPNW (d).

TABLE 3 Optimization of reaction conditions for aerobic oxidation of aromatic hydrocarbons of petroleum naphtha catalysed by Au–MnO_2@PPNS, Ag–MnO_2@PPNS, Au–MnO_2@PPNW and Ag–MnO_2@PPNW[a]

					Selectivity (%)[b]	
Entry	**Catalyst**	**Amount of catalyst (g)**	**Time (h)**	**Conversion (%)[b]**	**Benzaldehyde**	**Others**
1	PPNS	0.10	12	Trace	—	—
2	Au–MnO_2	0.01	8	8	99	—
3	MnO_2@PPNS	0.11	8	17	99	—
4	Au–MnO_2@PPNS	0.11	5	33	87	13
5		0.09	5	15	89	11
6		0.07	5	7	88	12
7	Ag–MnO_2	0.01	8	6	99	—
8	Ag–MnO_2@PPNS	0.11	6	29	84	16
9		0.09	6	18	85	15
10		0.07	6	10	87	13
11	PPNW	0.10	12	Trace	—	—
12	MnO_2@PPNW	0.11	8	20	99	—
13	Au–MnO_2@PPNW	0.11	5	36	85	15
14		0.09	5	18	84	16
15		0.07	5	12	90	10
16	Ag–MnO_2@PPNW	0.11	6	31	89	11
17		0.09	6	16	91	9
18		0.07	6	9	92	8

[a] Reaction conditions: toluene (8.0 ml), air as oxidant, reflux.

[b] Conversion and selectivity determined by GC analysis.

eachsupport itself, in the absence of MnO_2, Au–MnO_2 and Ag–MnO_2, cannot catalyse the reaction. Entries 2, 4, 7, 8, 13 and 16 show that the aggregated catalyst can catalyse the oxidation of the starting material to the corresponding aldehyde but the conversions are very low. Thus by dispersing the catalysts on the surface of the supports the activity of the catalytic systems is increased by a considerable amount. Also, when the catalytic systems in which only MnO_2 nanostructures supported on PPNS and PPNW were used (entries 3 and 12), the activity is lower than that of the Au- and Ag-loaded systems (entries 4, 8, 13 and 16).

To extend the scope of the prepared catalysts, the aerobic oxidation of the three isomers of xylene to the corresponding aldehydes was carried out under reflux

TABLE 4 Aerobic oxidation of aromatic hydrocarbons of petroleum naphtha catalysed by Au–MnO_2@PPNS, Ag–MnO_2@PPNS, Au–MnO_2@PPNW and Ag–MnO_2@PPNW[a]

					Selectivity (%)[b]	
Entry	**Substrate**	**Catalyst**	**Time (h)**	**Conversion (%)[b]**	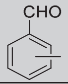	**Others**
1	*o*-Xylene	Au–MnO_2@PPNS	5	30	88	12
2		Ag–MnO_2@PPNS	6	29	91	9
3		Au–MnO_2@PPNW	5	31	87	13
4		Ag–MnO_2@PPNW	6	27	99	–
5	*m*-Xylene	Au–MnO_2@PPNS	5	21	96	4
6		Ag–MnO_2@PPNS	6	22	93	7
7		Au–MnO_2@PPNW	5	24	95	5
8		Ag–MnO_2@PPNW	6	19	90	10
9	*p*-Xylene	Au–MnO_2@PPNS	5	31	91	9
10		Ag–MnO_2@PPNS	6	30	92	8
11		Au–MnO_2@PPNW	5	31	82	18
12		Ag–MnO_2@PPNW	6	28	79	21

[a] Reaction conditions: arene (8.0 ml), Au–MnO_2@PPNS (0.11 g), Ag–MnO_2@PPNS (0.11 g), Au–MnO_2@PPNW (0.11 g), Ag–MnO_2@PPNW (0.11 g), air as oxidant, reflux.

[b] Conversion and selectivity determined by GC analysis.

TABLE 5 Oxidative synthesis of 2-arylbenzo[*d*]thiazole, 2-aryl-1*H*-benzo[*d*]imidazole and 2-aryl-4-quinazolinone derivatives[a]

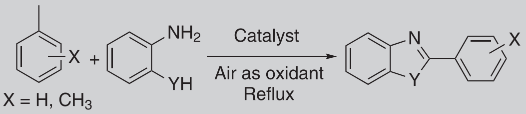

Entry	Y	Arene	Catalyst	Time (h)	Product	Yield (%)[b]	M.p. (°C)	
							Found	Reported
1	S	Toluene	Au–MnO$_2$@PPNS	2	**3a**	69	108–109	110–112[26]
2			Ag–MnO$_2$@PPNS	3		62		
3			Au–MnO$_2$@PPNW	2		67		
4			Ag–MnO$_2$@PPNW	3		59		
5	NH		Au–MnO$_2$@PPNS	2	**4a**	61	289–290	292–293[27]
6			Ag–MnO$_2$@PPNS	3		60		
7			Au–MnO$_2$@PPNW	2		59		
8			Ag–MnO$_2$@PPNW	3		55		
9	CONH		Au–MnO$_2$@PPNS	5	**5a**	76	231–233	232–235[28]
10			Ag–MnO$_2$@PPNS	7		72		
11			Au–MnO$_2$@PPNW	5		79		
12			Ag–MnO$_2$@PPNW	7		68		
13	S	*o*-Xylene	Au–MnO$_2$@PPNS	2	**3b**	62	55–56	55–57[29]
14			Ag–MnO$_2$@PPNS	3		61		
15			Au–MnO$_2$@PPNW	2		66		
16			Ag–MnO$_2$@PPNW	3		67		
17	NH		Au–MnO$_2$@PPNS	2	**4b**	53	223–225	223–224[27]
18			Ag–MnO$_2$@PPNS	3		50		
19			Au–MnO$_2$@PPNW	2		52		
20			Ag–MnO$_2$@PPNW	3		48		
21	CONH		Au–MnO$_2$@PPNS	5	**5b**	68	211–212	212–215[28]
22			Ag–MnO$_2$@PPNS	7		59		
23			Au–MnO$_2$@PPNW	5		67		
24			Ag–MnO$_2$@PPNW	7		65		
25	S	*m*-Xylene	Au–MnO$_2$@PPNS	2	**3c**	46	66–68	67–68[26]
26			Ag–MnO$_2$@PPNS	3		37		
27			Au–MnO$_2$@PPNW	2		42		
28			Ag–MnO$_2$@PPNW	3		40		
29	NH		Au–MnO$_2$@PPNS	2	**4c**	40	232–234	231–232[27]
30			Ag–MnO$_2$@PPNS	3		34		
31			Au–MnO$_2$@PPNW	2		39		
32			Ag–MnO$_2$@PPNW	3		37		
33	CONH		Au–MnO$_2$@PPNS	5	**5c**	49	209–210	210–211[30]
34			Ag–MnO$_2$@PPNS	7		44		
35			Au–MnO$_2$@PPNW	5		51		
36			Ag–MnO$_2$@PPNW	7		40		
37	S	*p*-Xylene	Au–MnO$_2$@PPNS	2	**3d**	74	85–86	86[26]
38			Ag–MnO$_2$@PPNS	3		71		
39			Au–MnO$_2$@PPNW	2		79		
40			Ag–MnO$_2$@PPNW	3		73		
41	NH		Au–MnO$_2$@PPNS	2	**4d**	70	275–277	275–276[27]
42			Ag–MnO$_2$@PPNS	3		64		
43			Au–MnO$_2$@PPNW	2		67		
44			Ag–MnO$_2$@PPNW	3		68		

(*Continues*)

TABLE 5 (Continued)

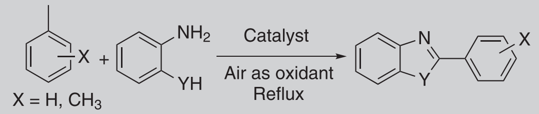

Entry	Y	Arene	Catalyst	Time (h)	Product	Yield (%)[b]	M.p. (°C)	
							Found	Reported
45	CONH		Au–MnO$_2$@PPNS	5	**5d**	87	229–230	231–234[28]
46			Ag–MnO$_2$@PPNS	7		76		
47			Au–MnO$_2$@PPNW	5		83		
48			Ag–MnO$_2$@PPNW	7		79		

[a]Reaction conditions: arene (10 ml), amine source (1.0 mmol), catalyst (0.11 g), air as oxidant, reflux.

[b]Isolated yield.

conditions and blowing air, using Au–MnO$_2$@PPNS, Ag–MnO$_2$@PPNS, Au–MnO$_2$@PPNW and Ag–MnO$_2$@PPNW catalysts (Table 4).

Because the aerobic oxidation of the aromatic hydrocarbons of petroleum naphtha (toluene and xylenes) can be carried out effectively using the prepared Au–MnO$_2$@PPNS, Ag–MnO$_2$@PPNS, Au–MnO$_2$@PPNW and Ag–MnO$_2$@PPNW catalysts, the transformation of inert substances (toluene and xylenes) into reactive substrates as precursors in one-pot tandem synthetic processes was examined using the four catalytic systems (Scheme 3). Consequently, Au–MnO$_2$@PPNS, Ag–MnO$_2$@PPNS, Au–MnO$_2$@PPNW and Ag–MnO$_2$@PPNW as effective aerobic oxidation catalysts were used in the tandem oxidative synthesis of 2-arylbenzo[*d*]thiazole, 2-aryl-1*H*-benzo[*d*]imidazole and 2-aryl-4-quinazolinone compounds using the aromatic hydrocarbons of petroleum naphtha as precursors (Table 5).

The recyclability of Au–MnO$_2$@PPNS, Ag–MnO$_2$@PPNS, Au–MnO$_2$@PPNW and Ag–MnO$_2$@PPNW was studied in the aerobic oxidation of toluene. The recovery of the catalysts from the reaction media was done using simple filtration. After washing the catalyst with ethanol (3 × 10 ml) it was dried in an oven. The recovered catalyst was used in the reaction as before. This process was done four successive times to evaluate the recyclability of the catalysts. The results (Figure 7) imply that the catalysts are usable for the reaction after recycling and no considerable decrease in the conversion is observed.

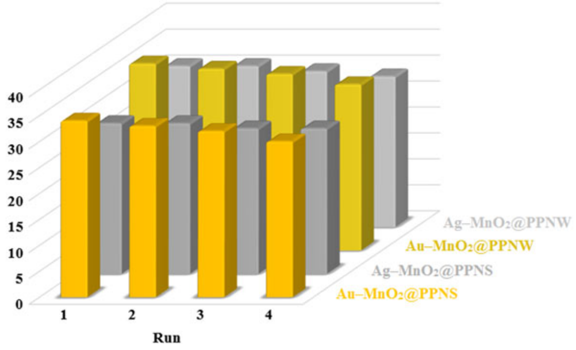

FIGURE 7 Successive use of Au–MnO$_2$@PPNS, Ag–MnO$_2$@PPNS, Au–MnO$_2$@PPNW and Ag–MnO$_2$@PPNW catalysts for the aerobic oxidation of toluene.

4 | CONCLUSIONS

Four novel catalytic systems (Au–MnO$_2$@PPNS, Ag–MnO$_2$@PPNS, Au–MnO$_2$@PPNW and Ag–MnO$_2$@PPNW) for the conversion of the inert aromatic hydrocarbons of petroleum naphtha to active materials in the tandem oxidative synthesis of organic compounds were reported. The Au–MnO$_2$@PPNS, Ag–MnO$_2$@PPNS, Au–MnO$_2$@PPNW and Ag–MnO$_2$@PPNW catalytic systems were used successfully in the synthesis of 2-arylbenzo[*d*]thiazole, 2-aryl-1*H*-benzo[*d*]imidazole and 2-aryl-4-quinazolinone derivatives. The distribution of Au–MnO$_2$ and Ag–MnO$_2$ nanostructures on the surface of PPNS and PPNW gave more active catalytic systems in comparison to the aggregated catalysts. In the presented procedures, air was used as an inexpensive oxidant which can be used without the need for additional oxidants. The renewability, biodegradability and recyclability are other advantages of the Au–MnO$_2$@PPNS, Ag–MnO$_2$@PPNS, Au–MnO$_2$@PPNW and Ag–MnO$_2$@PPNW catalytic systems.

ACKNOWLEDGEMENTS

We gratefully acknowledge the financial support from the Iran National Science Foundation (INSF) and Research Council of Shahid Beheshti University.

REFERENCES

[1] R. Nie, J. Shi, S. Xia, L. Shen, P. Chen, Z. Hou, F.-S. Xiao, *J. Mater. Chem.* **2012**, *22*, 18115.

[2] R. J. K. Taylor, M. Reid, J. Foot, S. A. Raw, *Acc. Chem. Res.* **2005**, *38*, 851.

[3] J. Wan, L. Zhou, H. Deng, F. Zhan, R. Zhang, *J. Mol. Catal. A* **2015**, *407*, 67.

[4] G. Harichandran, S. D. Amalraj, P. Shanmugam, *J. Mol. Catal. A* **2014**, *392*, 31.

[5] M. Das, K. G. Bhattacharyya, *J. Mol. Catal. A* **2014**, *391*, 121.

[6] X. Li, J. Liu, Y. Zhao, H. Zhang, F. Du, C. Lin, T. Zhao, Y. Sun, *ChemCatChem* **2015**, *7*, 1848.

[7] W. Wei, X. Cui, W. Chen, D. G. Ivey, *Chem. Soc. Rev.* **2011**, *40*, 1697.

[8] J. Kang, A. Hirata, L. Kang, X. Zhang, Y. Hou, L. Chen, C. Li, T. Fujita, K. Akagi, M. Chen, *Angew. Chem. Int. Ed. Engl.* **2013**, *52*, 1664.

[9] S. Jana, S. Pande, A. K. Sinha, S. Sarkar, M. Pradhan, M. Basu, S. Saha, T. Pal, *J. Phys. Chem. C* **2009**, *113*, 1386.

[10] R. K. Kunkalekar, A. V. Salker, *Catal. Commun.* **2010**, *12*, 193.

[11] K. Mette, A. Bergmann, J.-P. Tessonnier, M. Hävecker, L. Yao, T. Ressler, R. Schlögl, P. Strasser, M. Behrens, *ChemCatChem* **2012**, *4*, 851.

[12] R. Averlant, S. Royer, J.-M. Giraudon, J.-P. Bellat, I. Bezverkhyy, G. Weber, J.-F. Lamonier, *ChemCatChem* **2014**, *6*, 152.

[13] G. Zhang, L. Zheng, M. Zhang, S. Guo, Z.-H. Liu, Z. Yang, Z. Wang, *Energy Fuels* **2012**, *26*, 618.

[14] J. Chen, K. Vongsanga, X. Wang, N. Byrne, *Materials (Basel)* **2014**, *7*, 6158.

[15] J. P. Paraknowitsch, J. Zhang, D. Su, A. Thomas, M. Antonietti, *Adv. Mater.* **2010**, *22*, 87.

[16] S. Y. Cho, Y. S. Yun, S. Lee, D. Jang, K.-Y. Park, J. K. Kim, B. H. Kim, K. Kang, D. L. Kaplan, H.-J. Jin, *Nat. Commun.* **2015**, *6*, 7145.

[17] P. E. Ingham, *J. Appl. Polym. Sci.* **1971**, *15*, 3025.

[18] C. Popescu, E. Segal, C. Iditoiu, *Thermochim. Acta* **1995**, *256*, 419.

[19] A. Shaabani, P. Mirzaei, S. Naderi, D. G. Lee, *Tetrahedron* **2004**, *60*, 11415.

[20] A. Shaabani, Z. Hezarkhani, S. Shaabani, *RSC Adv.* **2014**, *4*, 64419.

[21] A. Shaabani, Z. Hezarkhani, E. Badali, *RSC Adv.* **2015**, *5*, 61759.

[22] A. Shaabani, Z. Hezarkhani, E. Badali, *RSC Adv.* **2015**, *5*, 91966.

[23] A. Shaabani, Z. Hezarkhani, E. Badali, *Polyhedron* **2016**, *107*, 176.

[24] S. Xu, L. Yong, P. Wu, *ACS Appl. Mater. Interfaces* **2013**, *5*, 654.

[25] A. Idris, R. Vijayaraghavan, U. A. Rana, A. F. Patti, D. R. MacFarlane, *Green Chem.* **2014**, *16*, 2857.

[26] Q. Song, Q. Feng, M. Zhou, *Org. Lett.* **2013**, *15*, 5990.

[27] D. Mahesh, P. Sadhu, T. Punniyamurthy, *J. Org. Chem.* **2015**, *80*, 1644.

[28] H. Hikawa, Y. Ino, H. Suzuki, Y. Yokoyama, *J. Org. Chem.* **2012**, *77*, 7046.

[29] M. Bala, P. K. Verma, U. Sharma, N. Kumar, B. Singh, *Green Chem.* **2013**, *15*, 1687.

[30] J. Zhou, J. Fang, *J. Org. Chem.* **2011**, *76*, 7730.

SUPPORTING INFORMATION

Additional Supporting Information may be found online in the supporting information tab for this article.

How to cite this article: Hezarkhani, Z., and Shaabani, A. (2016), Au- and Ag-loaded MnO_2 nanostructures supported on nitrogen- and nitrogen–sulfur-doped pyroproteins: Synthesis and catalytic activity in organic transformations, *Appl. Organometal. Chem.*, doi: 10.1002/aoc.3624